Journal of Solid State Chemistry **143,** 115–121 (1999)
Article ID jssc.1998.8092, available online at http://www.idealibrary.com on IDEAL®

Method for Calculating Ionic and Electronic Defect Concentrations in Proton Containing Perovskites

Finn Willy Poulsen

Materials Research Department, Risø National Laboratory, DK-4000 Roskilde, Denmark

Received July 15, 1998; in revised form November 7, 1998; accepted November 8, 1998

A general numerical method for calculation of concentrations of vacancies and ionic and electronic defects in solids in equilibrium with two gas pressures is presented. The method is applied to 5 at% B-site doped $SrCeO_3$ in equilibrium with oxygen and water vapor. The model includes protons and electronic defects, as well as cation vacancies on the *A* and *B* sites. The 10 concentrations in the model are determined uniquely by solving the linear and mass action law type equations in a rational sequence. No approximations or truncations of the equations are necessary. No information on the magnitude of the Schottky-equilibrium constant, K_s, controlling the population of cation vacancies is available. Limiting values of K_s were tested to illustrate suppression and enhancement of cation vacancy formation in perovskites. Deviations from Sieverts law are demonstrated. Deviation of the *A*/*B* ratio from unity has the same effect on the proton content as an increase of the dopant level. © 1999 Academic Press

Key Words: **Brouwer diagram; calculation; trial and error; protonic; electronic; defects; perovskite.**

INTRODUCTION

The traditional strategies for defect concentration calculations on doped, mixed conducting oxides rely on (i) omission of concentration terms from the electroneutrality equation for species of low concentration and (ii) assumptions for certain (high) concentrations of the host ions or oxygen vacancies, namely, that these are virtually independent of the partial pressure of oxygen. The analytical expressions one derives using these approximations are seldom of higher order than cubic. A typical approximative approach is employed in Ref. (1) for doped ceria. Approximation methods describe well the defect chemistry in regions of oxygen partial pressure, where predominantly *p*-type, predominantly ionic, or predominantly *n*-type behavior is observed. The procedure, however, fails to describe regions over one to three decades of oxygen partial pressure, where transitions from one defect type regime to the next take place. The approximation procedure becomes questionable with regard both to pedagogical value and to precision, when the defect chemistry of the solid is established by equilibration with two or more gases. Along the same line, Schottky-type equilibria involving more than two types of ions, such as the chemical equilibrium for perovskites associated with Eq. [7], are never considered in approximative solutions, since such third or higher order expressions in concentration are rather intractable to approximations. Nowotny and Rekas (2) recently modeled sub- and over stoichiometric (in oxygen) $(La,Sr)MnO_3$, but their solution is only valid under the restriction that $[V^{\cdot\cdot\cdot}_{La}] = [V^{\cdot\cdot\cdot}_{Mn}]$; i.e., it only applies to the case where the *A*/*B*-ratio equals unity. Commercial equation solving codes can in principle solve all defect, mass balance, and electroneutrality equations simultaneously by minimizing the residuals of the equations; see Ref. (3). The author's experience is that such codes often diverge or oscillate, since some of the partial pressures and concentrations are extremely small, while other concentrations simultaneously are large. Complete analytical expressions, obtained by substituting the linear equations into the nonlinear mass action law expressions will unavoidably lead to polynomials of high order in the unknown concentrations. An example of an exact defect description of a proton containing perovskite, resulting in a fourth degree polynomium, is presented by Bonanos and Poulsen in Ref. (4). However, as a general approach, the derivation of analytical, high order analytical expression (which would have to be solved by numerical means anyhow) appears therefore not to furnish a practical strategy.

The present procedure is general and calculates the concentrations in a stepwise manner, identifying the correct set of concentrations by a screening test. The partial pressure of oxygen, or alternatively of water vapor, corresponding to such a set of concentrations is finally calculated. This method was successfully used by us in 1993 on the *B*-site-doped perovskite $NdCr_{1-x}Ti_xO_{3\pm\delta}$ (5).We demonstrated in 1997 the applicability of the method to the more complex case of simultaneous presence of protonic, oxidic, and electronic defects in fluorite structure oxides (6). A similar mathematical principle was used by Spinolo and Anselmi-Tamburini in 1995 (7) to calculate defect concentrations in

0022-4596/99 $30.00

MO_2 oxides with interstitial cations having charges from 0 to +4. A more generalized treatment was given by Spinolo *et al.* in 1997 (8).

MATHEMATICAL FOUNDATION OF THE METHOD

(i) A model is formulated containing N different ionic and electronic species (neutral or charged); The Kröger–Vink notation (9) is used in the present paper. The word "species" means in the following any ion, neutral atom, electron- or electron hole defect and vacancy in the solid, including the proton attached to a lattice oxygen; cf. Table 1.

(ii) N independent equations are derived from mass balances, site balances, the electroneutrality condition, internal ionic and electronic equilibria, and finally equilibria between the solid sample and the gas atmosphere (typically equilibria with oxygen and/or water vapor). This set of equations is checked for presence of redundant equations (linear combinations of the other equations). Until this point we have followed a traditional route.

(iii) The calculation algorithm requires a species to be selected, the concentration of which will traverse several orders of magnitude, as the partial pressure of oxygen and/or water vapor is varied. It is a further functional requirement that the concentration of this species must vary monotonically with the gas pressure. At least four lattice species behave in this manner: There must exist a monotonic relation between the pO_2 of a gas in equilibrium with an oxide and the chemical potential of oxygen in the solid (and therefore also some monotonic relationship to the "chemical activity" of oxygen vacancies); similarly one can assume that the electron and electron hole concentrations bear a monotonic relationship to the reducing/oxidizing potential of the gas equilibrating with the solid. In the case of protonic and electronic defects in fluorite structure oxides, the electron hole concentration was most conveniently chosen as the running parameter. In the case of perovskites with inclusion of cation vacancies we use the oxygen vacancy concentration, $[V_O^{\bullet\bullet}]$ (see the following sections). For generality, let this species be named i, and let the concentration interval of interest for species i be $\min < [i] < \max$. We will find solutions for all concentrations of the other species corresponding to a selection of values of $[i]$ in this interval. It is convenient to vary $[i]$ in logarithmic steps through the interval $\min < [i] < \max$. By fixing one concentration within its physically possible interval, we have in effect added one (simple linear) equation to the set of N equations. We are therefore free to "avoid" one of the more problematic equations, which will typically be one of the high order mass action law expressions. An alternative way of explaining the basis of the present method is formulated as follows: In a series of physicochemical measurements on a non-stoichiometric oxide we normally consider temperature and partial pressure of oxygen as independent variables (controlled by the operator) and the concentrations as the dependent variables. The latter statement relates solely to a statistical treatment. From a computational point of view, however, one is free to select any two parameters as independent variables (here we choose one temperature, which in turn fixes all equilibrium constants and *one* concentration), if this makes the calculation simpler.

(iv) If the solid is in equilibrium with two different gasses, of pressure p_1 and p_2, respectively, we will identify solutions for discrete values of p_1 in the interval $p_{\min} < p_1 < p_{\max}$. Thus p_1 will be fixed for each trial and error calculation of the concentrations. A number of the N equations identified under (ii) are linear. By insertion of $[i]$ into these, we find some of the other concentrations. Substitution of the remaining linear equations into properly selected mass law expressions leads to quadratic equations, which are solved analytically. Eventually all concentrations are found by this procedure. What remains is to ensure that the concentrations are positive and below their maximum allowed magnitude (e.g., in crystals, a site cannot be more than 100% occupied). Invalid solution sets will disqualify themselves by containing one or more negative, complex, or too large positive roots among the calculated N concentrations. The approved set of concentrations are inserted into the equation having the highest order, which has not yet been employed (typically the equilibrium expression for reaction with oxygen). Thereby the corresponding $p_2 = pO_2$ is found.

TABLE 1
Simplest Realistic Defect Model for B-Site Doped $SrCeO_3$

A site	*B* site	O site	Delocalized
$Sr_A^{\times}$	$Ce_B^{\times}$	$O_O^{\times}$	$h^{\bullet}$
$V_A^{\prime\prime}$	$Y_B^{\prime}$	$V_O^{\bullet\bullet}$	$e^{\prime}$
	$V_B^{\prime\prime\prime\prime}$	$OH_O^{\bullet}$	

Note. The dopant, Y, is assumed to be trivalent.

APPLICATION TO DOPED STRONTIUM CERATE

A- and/or *B*-site-doped perovskites can in principle exist in both an over- and an understoichiometric state depending on the redox properties of the *A* and *B* ions, temperature, and partial pressure of oxygen. The present model is made general in order to take account of this: in the over-stoichiometric regime cation vacancies have to be assumed, as verified in doped and undoped $LaMnO_{3+\delta}$ by neutron diffraction (10) and oxygen content measurements (11). There is no room for interstitial oxygens in a perovskite structure. The model is furthermore made complete by including protonic species. Doped $SrCeO_3$ and, in more

recent years, also Sr- and Ca-zirconates have been intensely studied by Iwahara and co-workers (12,13) as a new class of high-temperature protonic conductors. Table 1 summarizes the species in the general model, using the Kröger–Vink notation with the ionic charges of $Sr(II)Ce(IV)O_3$ as the reference state. It requires 10 different "species" in the present model to describe fully the defect chemistry of $Sr_zCe_{1-x}Y_xO_{3-x/2\pm\delta}H_\varepsilon$. Protons are residing on lattice oxygens, $OH_O^\bullet$, in the present description. The site conservation equation [3] would have to be modified if protons were assigned an individual "life" as interstitial protons, $H_i^\bullet$.

The 10 independent equations, describing the system uniquely, are as follows. Note the special notation for concentrations of electronic defects: concentration of holes $[h^\bullet]$ is denoted 'p'; concentration of electrons $[e^{|}]$ is given by n in the equations below.

Site balances:

$$\text{Sr site} \quad [Sr_A^\times] + [V_A^{||}] = 1 \qquad [1]$$

$$\text{Ce site} \quad [Ce_B^\times] + [Y_B^{|}] + [V_B^{||||}] = 1 \qquad [2]$$

$$\text{Oxide site} \quad [V_O^{\bullet\bullet}] + [O_O^\times] + [OH_O^\bullet] = 3. \qquad [3]$$

Mass balances:

$$[Ce_B^\times]/[Y_B^{|}] = (1-x)/x \qquad [4]$$

$$A/B \text{ ratio} \equiv [Sr_A^\times]/([Ce_B^\times] + [Y_B^{|}]) = z. \qquad [5]$$

Electroneutrality condition:

$$2\cdot[V_A^{||}] + [Y_B^{|}] + 4\cdot[V_B^{||||}] + n = 2\cdot[V_O^{\bullet\bullet}] + [OH_O^\bullet] + p. \qquad [6]$$

Mass action laws:

Schottky reaction for vacancy generation:

$$\text{nil} \leftrightarrow 3\,V_O^{\bullet\bullet} + V_A^{||} + V_B^{||||}$$

$$\Rightarrow [V_O^{\bullet\bullet}]^3\cdot[V_A^{||}]\cdot[V_B^{||||}] = K_s. \qquad [7]$$

Internal electronic equilibrium:

$$K_i = n\cdot p \qquad [8]$$

Equilibria between the solid sample and the gas atmosphere:

$$\tfrac{1}{2}O_2\,(\text{gas}) + V_O^{\bullet\bullet} \leftrightarrow O_O^\times + 2h^\bullet$$

$$\Rightarrow K_{ox} = [O_O^\times]\cdot p^2/(pO_2^{1/2}\cdot[V_O^{\bullet\bullet}]) \qquad [9]$$

$$H_2O(\text{gas}) + V_O^{\bullet\bullet} + O_O^\times \leftrightarrow 2OH_O^\bullet$$

$$\Rightarrow K_w = [OH_O^\bullet]^2/(pH_2O\cdot[V_O^{\bullet\bullet}]\cdot[O_O^\times]). \qquad [10]$$

The solutions for the cation concentrations are not trivial when cation vacancies are included. The 10 equations group into 6 linear expressions and 4 nonlinear ones. An analytical expression in one of the concentrations could in principle be obtained by substitution; it would probably result in a polynomium of the 6′–9′ degree for this model. It is demonstrated below that the system of equations can be solved in a simple way, assuming a smart strategy is applied.

We want to carry out a calculation for known values of the four equilibrium constants, Eqs. [7]–[10], and for a known dopant level x and A/B ratio $= z$. We furthermore specify a number of pH_2O values, at which the calculation is required.

The stepwise calculation proceeds as follows: We assume a value for $[V_O^{\bullet\bullet}]$ and pH_2O.

By substituting Eq. [10] into Eq. [3] one obtains a quadratic equation in $[OH_O^\bullet]$ reading

$$[OH_O^\bullet]^2/([V_O^{\bullet\bullet}]\cdot pH_2O\cdot K_w) + [V_O^{\bullet\bullet}] + [OH_O^\bullet] - 3 = 0. \qquad [11]$$

Equation [11] is solved analytically.

$[O_O^\times]$ is then found from Eq. [3]:

$$[O_O^\times] = 3 - [V_O^{\bullet\bullet}] - [OH_O^\bullet]. \qquad [3']$$

The next task is to express $[V_B^{||}]$ and $[V_B^{||||}]$ by $[Y_B^{|}]$ making use of Eqs. [1], [2], and [4] and to insert these in Eq. [7]. The resulting expression in $[Y_B^{|}]$ is still only of second order in $[Y_B^{|}]$:

$$(1 - z\cdot[Y_B^{|}]/x)\cdot(1 - [Y_B^{|}]/x) = K_s/[V_O^{\bullet\bullet}]^3. \qquad [12]$$

The positive (analytical) solution for $[Y_B^{|}]$ of Eq. [12] leads to

$$[V_A^{||}] = 1 - z\cdot[Y_B^{|}]/x \quad \text{and} \quad [V_B^{||||}] = 1 - [Y_B^{|}]/x \qquad [13,14]$$

The solutions for the host ions follow immediately from [1], [2]:

$$[Ce_B^\times] = 1 - [V_B^{||||}] - [Y_B^{|}] \text{ and } [Sr_A^\times] = 1 - [V_A^{||}]. \qquad [1',2']$$

At this point only the values of n, p and the corresponding pO_2 remain to be determined. In the electroneutrality equation [6], n can be replaced by K_i/p from Eq. [8]:

$$2\cdot[V_A^{||}] + [Y_B^{|}] + 4\cdot[V_B^{||||}] + K_i/p = 2\cdot[V_O^{\bullet\bullet}] + [OH_O^\bullet] + p. \qquad [6']$$

Equation [6′] is again only a quadratic expression in p; all other terms have known numerical values. Equation [6′] is

solved for p. The electron concentration, n, is finally found from [8] as

$$n = K_i/p. \qquad [8']$$

So far we have not employed Eq. [9], since we initially "replaced" it by the linear equation $[V_O^{\bullet\bullet}]$ = an assumed numerical value. The three concentrations entering Eq. [9] define the partial pressure of oxygen corresponding to the set of 10 determined concentrations, assuming they all are within the physically possible range. We can thus accept the solution if the concentration of the ith species fulfils $0 < [i] < 1$ for $[Y_B^{|}]$, $[V_A^{||}]$, $[V_B^{||||}]$, $[Ce_B^{\times}]$, $[Sr_A^{\times}]$, n and p; and $0 < [i] < 3$ for $[V_O^{\bullet\bullet}]$, $[O_O^{\times}]$, and $[OH_O^{\bullet}]$. If the set of concentrations is accepted, we can insert $[V_O^{\bullet\bullet}]$, $[O_O^{\times}]$, and p into [9] and find the oxygen partial pressure that corresponds to the equilibrium concentrations. The calculation is next performed for a new value of $[V_O^{\bullet\bullet}]$. When $[V_O^{\bullet\bullet}]$ has covered the concentration interval of interest, we change to a new value of pH_2O and start all over again. The complete calculation of a three-dimensional Brouwer diagram (10 concentrations versus pH_2O and pO_2 for some 10×30 points in the pH_2O–pO_2 plane) took initially 20–30 s, programmed in primitive GWbasic and performed on a 486 PC. In a Pascal version the calculation takes less than 1 s. A printout of the program source code fills less than two A4 pages. An Excel spreadsheet version is available from the author.

DISCUSSION

General Performance of the Algorithm

The algorithm is built on three loops: in the outermost loop the program calculates for a set of Y-dopant concentrations and/or A/B ratios; for each doping level typically 6–12 pH_2O values are calculated, typically in the range 10^{-6} to 1 atm; in the innermost cycle 500–1000 steps of $[V_O^{\bullet\bullet}]$ in the interval $10^{-14} - 0.5$ are tested. The simulation thus stops at an oxygen content corresponding to the Brownmillerite composition $ABO_{2.5}$. In order to obtain satisfactory numerical precision, all variables in the algorithm must be declared as double precision variables. Some intuition is mandatory in order to find the right sequence in which the concentrations are calculated: very small concentrations should be calculated from mass action law expressions rather than from linear difference equations. A test, comparing the left-hand side and the right-hand side of the electroneutrality condition (Eq. [6]), reveals cumulative errors, which are usually around 10^{-14} to 10^{-18} atomic fraction.

Several features of the present procedure are evident: (i) simulations can be carried out to "dangerous" or "non-physical" high pressures; (ii) smooth transitions extending over several decades of pO_2 from one defect regime to the next are observed—this being in contrast to the "too straight" lines usually seen in hand-drawn Brouwer diagrams; (iii) very small, but finite stoichiometry deviations can be predicted. A few drawbacks of the present procedure must admittedly be exposed: (i) The calculated defect concentrations will result in a set of discrete oxygen pressures, the magnitude of which cannot be controlled; (ii) using logarithmic steps in $[V_O^{\bullet\bullet}]$ generates relatively few calculated points in those (intermediate) pO_2 regimes, where the oxygen stoichiometry varies little; however, Brouwer diagrams do not usually have unexpected features in such regions anyhow.

Defect schemes are often tested at the high and low extremes of oxygen partial pressures by plotting the logarithm of the measured total conductivity versus the logarithm of pO_2. The predicted slope, $\partial \log(\sigma)/\partial \log(pO_2)$, is traditionally derived from approximations to Eqs. [9] (in combination with Eqs. [8] at low partial pressures). For the doped perovskite structures one arrives at slopes of $+1/4$ and $-1/4$ (for the non-doped case $\pm 1/6$).

"Differentiated" Brouwer diagrams can easily be generated as output from the present simulations. $\Delta \log[i]/\Delta \log(pO_2)$ calculated between adjacent points is a sufficiently good approximation to $\partial \log[i]/\partial \log(pO_2)$ assuming calculated points lie close. Figure 5 shows such a plot. It is noted that deviations from the "magic" slopes occur for p and n at low pO_2. The region of $\partial \log[V_O^{\bullet\bullet}]/\partial \log(pO_2) = 0$ between 1 and 10^{-15} atm is the region of constant oxygen stoichiometry. The use of "differentiated" Brouwer diagrams is hereby advocated. The algorithm for this model system can, without modifications, be used to model perovskites, where protons have no or negligible solubility. This is achieved by setting $K_w \equiv 0$.

Actual Simulations

The equilibrium constants for $SrCe_{0.95}Yb_{0.05}O_{3\pm d}$ at 700°C, employed by Schober and Wenzl (14), were adjusted to the present definitions of the equilibrium constants. The values are $K_{ox} = 3 \cdot K_1 = 1.5 \times 10^{-5}$ $(atm)^{-1/2}$, $K_i = 10^{-11}$, and $K_w = 10$ $(atm)^{-1/2}$.

The present model is probably the first attempt to formulate a complete model for the defect chemistry of proton containing perovskites *including* cation vacancies. The factors controlling cation vacancy concentrations have therefore to be discussed in the following.

The inclusion of cation vacancies is described by a Schottky equilibrium (Eq. [7]). Cation vacancy formation will in general be favored by increasing temperature for entropic reasons; i.e., it is predicted that K_s increases with temperature. This is counteracted by the fact that oxygen vacancy formation via reaction [9] is probably also promoted by increasing temperature. A certain concentration of cation vacancies can in addition deliberately be imposed on the system by synthesis of materials with A/B ratios

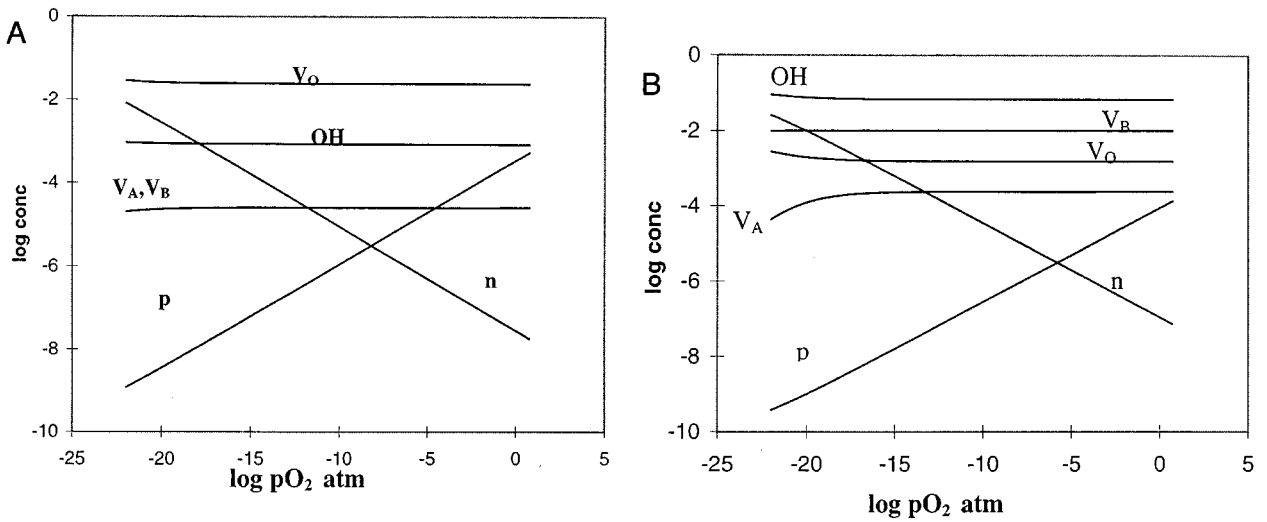

FIG. 1. Proton and other defect concentrations as function of pO_2, at 700°C. $K_s = 10^{-14}$, $K_{ox} = 1.5 \times 10^{-5}$, $K_i = 110^{-11}$, $K_w = 10$. Dopant level $x = 0.05$. (A) A/B ratio = 1.0 and $pH_2O = 10^{-6}$ atm; (B) A/B ratio = 0.99 and $pH_2O = 10^{-2}$ atm.

deviating from unity. Large concentrations of *B*-site vacancies are, however, probably not possible due to the high local charge on the *B*-site vacancy/ion. If a certain (as yet unknown) concentration is exceeded, breakdown of the perovskite structure will occur, resulting in formation of new phases. Equation (7) can thus be visualized as a sort of solubility product. Large concentrations of oxygen vacancies are possible, as in the disordered, high-temperature phase of $SrFeO_{2.5+d}$ (Brownmillerite structure at low temperature). In the latter material up to 17% of the oxygen sites are empty. Similarly, structures with large deficits of *A* ions can be derived from perovskites, e.g., WO_3, where there are no *A* ions needed at all to stabilize the structure.

Only a few reports have been found where the variation of the A/B ratio in perovskites with Ce on the *B* site has been addressed experimentally. Shima and Haile (15) investigated undoped and Gd-doped $BaCeO_3$, with A/B ratios ranging from 0.96 to 1.04. In some cases *A*-site-deficient-materials were obtained due to loss of BaO during the high-temperature treatment. Ahlgren *et al.* (16) studied the sintering and electrical properties of Y-doped $SrCeO_3$ with A/B ratios ranging from 0.990 to 1.005 (in steps of 0.005) and found that the best ceramic was obtained with $A/B = 0.995$. However, no information on the magnitude of K_s is available. Test calculations show that a value for $K_s = 10^{-20}$ or lower corresponds to a neglegible tendency to cation vacancy formation, while, for instance, $K_s = 3.2 \times 10^{-9}$ corresponds to coexistence of approximately 2 at % of $V_O^{\bullet\bullet}$, $V_A^{\|}$ and $V_B^{\|\|\|}$. Figure 1A shows a representative Brouwer diagram for a 5% Yb-doped strontium cerate at 700°C and a water partial pressure of 10^{-6} atm. The Schottky equilibrium, allowing formation of cation vacancies, has been included with $K_s = 10^{-14}$. The calculated cation vacancy concentrations are around 3×10^{-5} atomic fraction; the *A*- and *B*-site vacancy concentrations are equal, since the A/B ratio for this calculation is unity. The curves showing *n*- and *p*-type concentrations are symmetrical around a horizontal line passing through the point, where $n = p$ (at around $pO_2 = 10^{-8}$ atm). The proton content and $[V_O^{\bullet\bullet}]$ increase at low pO_2, which is more clearly illustrated in Figs. 2 and 3. The increase in protons at low pO_2 is a consequence of the increase in $[V_O^{\bullet\bullet}]$, giving room to more water uptake via reaction [10]. For a more detailed discussion of this effect, see Ref. (4). Figure 1B shows a calculation for the same values of equilibrium constants as in Fig. 1A, but the water

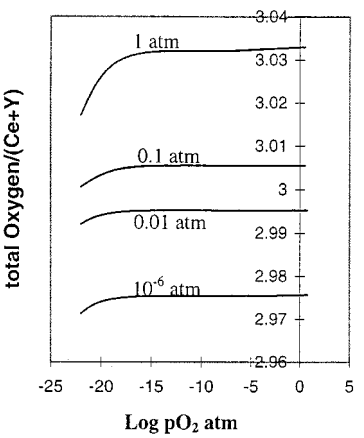

FIG. 2. Total oxygen content in a perovskite as function of partial pressure of oxygen for four water partial pressures in the range 10^{-6} to 1 atm. $K_s = 10^{-14}$, $K_{ox} = 1.5 \times 10^{-5}$, $K_i = 110^{-11}$, $K_w = 10$. A/B ratio = 1, dopant level $x = 0.05$.

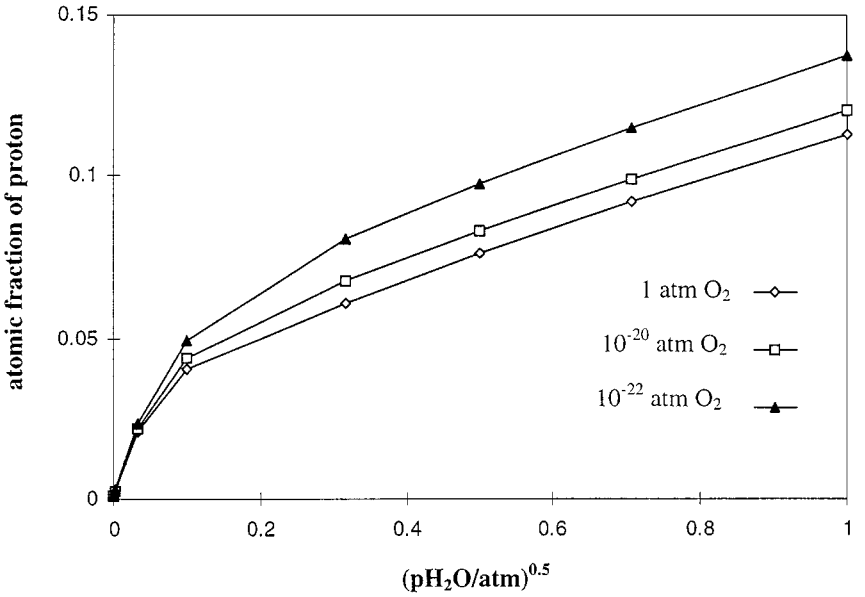

FIG. 3. Dependence of proton content (atomic fraction) on the square root of water partial pressure (atm) for three different oxygen partial pressures (atm). Values of equilibrium constants and composition are as in Fig. 2.

vapor pressure has been increased from 10^{-6} in Fig. 1A to 10^{-2} atm in Fig. 1B. At the same time the A/B ratio has been lowered to 0.99. Several things have happened: the proton concentration is now higher than the oxide ion vacancy concentration; the concentrations for the cation vacancies now follow two different curves—the B-site vacancy concentration is roughly a factor of 20 higher than the A-site vacancy concentration; and finally, the crossover pO_2, where $n = p$, has moved toward higher pO_2.

In situations far from saturation by protons, the proton content of the perovskite will sometimes follow the so-called Sieverts law, according to which the proton content is proportional to the square root of the partial pressure of water vapor. The law follows from Eq. [10], when one assumes $[V_O^{\bullet\bullet}]$ and $[O_O^{\times}]$ to be constant. In reality these two species are not constant in concentration, and the ratio of overall oxygen content to total amount of B ions does not have a general limiting value of $3 - [Y'_B]/2$. The pO_2 region,over which in a thermogravimetric experiment one observes a constant weight, therefore cannot be used as a reference point unless one has supplementary information. Figure 2 illustrates the predicted overall stoichiometry for partial pressures of water from 10^{-6} to 1 atm. The proton content increases monotonically with increasing pressure. Only at the lowest water partial pressure of 10^{-6} atm does one find that the limiting oxygen content is close to $3 - [Y'_B]/2 = 2.975$. Figures 3a and 3b in the paper of Schober and Wenzl (11) were supposed to illustrate this trend, but unfortunately show the results of a calculation corresponding to equilibrium constants different from those quoted in (11).

Figure 3 shows the protonic content as a function of the square root of the water partial pressure in the same range as in Fig. 2. Three deviations from "conventional" behavior are seen when cation vacancies are included in the defect model: (i) the proton content at high water partial pressure can exceed the doping level, here 0.05 atomic fraction; (ii) Sieverts law is obeyed only at very low partial pressure of water; (iii) a second linear regime in this square root plot is surprisingly also observed above 0.1 atm of pH_2O. Such an

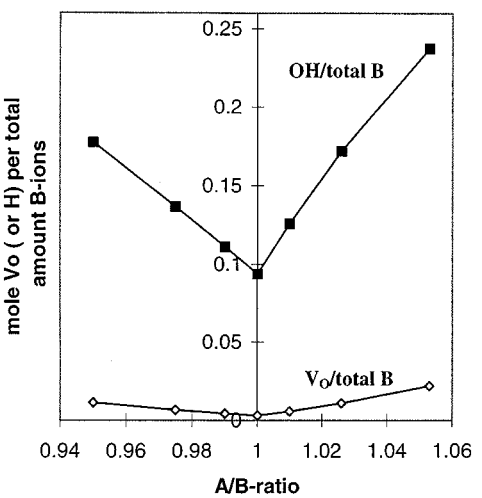

FIG. 4. Effect of A/B ratio on proton content and oxygen vacancy concentrations at $pH_2O = 1$ atm and 10^{-1} atm of pO_2; dopant level $x = 0.1$; $K_s = 0$. The concentrations have been normalized with respect to total amount of B ions in the solid.

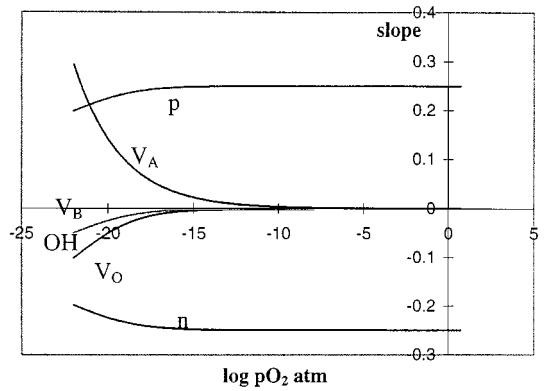

FIG. 5. Differentiated Brouwer diagram; data are the same as used for the generation of Fig. 1B. Slope is calculated for the various species, *i*, as $\delta \log [i]/\delta \log(pO_2)$.

observation could lead the experimenter to infer, by extrapolation to $pH_2O = 0$ atm, that the perovskite contains a certain amount (in the present case approximately 0.03 atomic fraction) of nonremovable protons.

Deviations of the A/B-ratio were finally modeled. Forcing the system to accomodate cation vacancies on either the A or B site has two effects: (i) The deficit of charge on the respective site has the same effect as if the system has been doped to a higher Y level. Fig. 4 shows the resulting concentrations of $[OH_O^{\bullet}]$ and $[V_O^{\bullet\bullet}]$ for A/B ratios in the range 0.950 to 1.053; (ii) The proton content is seen to increase as the A/B deviates from unity, the increase being approximately twice as strong for the B-ion-deficient regime. This is understandable since the ratio of the charges of $V_B^{|||}$ and $V_A^{||}$ is also equal to two. The equilibrium concentration of oxygen vacancies also increase slightly when the A/B ratio deviates from unity. The simulations furthermore show that materials with same doping level, but different A/B ratio, will, when compared at the same pO_2 and pH_2O, have very similar concentrations of hole carriers. Predictions and arguments based on isolated equilibria, such as the Schottky equilibrium, Eq. [7], in combination with Eq. [10] will inevitably lead to erroneous conclusions.

Extension to Other Defect Problems

Associates between oxygen vacancies and dopants/host ions were left out in the present treatment, due to complete ignorance regarding its importance in $SrCeO_3$-type materials. Test cases with strong association were examined by Schober and Wenzl (14). The present author will in the near future publish algorithms treating the following complex defect systems: (i) over- and understoichiometric perovskites such as $(La_{1-x}Sr_x)_yMnO_{3\pm\delta}$ with varying A/B ion ratios; (ii) Mg-doped $LiFeO_2$ (rock salt structure); (iii) defect association in doped and reduced ceria; and (iv) doped pyrochlore materials. At present the technique is being applied to modeling of the defect chemistry of the oxygen separation membrane material $Sr_4Fe_{6-x}Co_xO_{13\pm\delta}$ (17).

ACKNOWLEDGMENTS

The present work was started during the author's employment by The Nordic Energy Research Program for Fuel Cells, NEFP; continued under the Danish DK-SOFC projects; and completed with support and inspiration from the NEDO project on "Advanced Ceramics for Protonics, 1995–1998." Numerous fruitful discussions with N. Bonanos of Risø National Laboratory have assisted in the development of the present method.

REFERENCES

1. M. A. Panhans and R. N. Blumenthal, *Solid State Ionics* **60,** 279 (1993).
2. J. Nowotny and M. Rekas, *J. Am. Ceram. Soc.* **81**(1), 67 (1998).
3. T. Schober, W. Schilling and H. Wenzl, *Solid State Ionics* **86–88,** 653 (1996).
4. N. Bonanos and F. W. Poulsen, *J. Mater. Chem.* **9** (1999).
5. A. Holt, E. Ahlgren, and F. W. Poulsen, *in* "Proceedings, Third International SOFC, Honolulu" (S. C. Singhal and H. Iwahara, Eds.), Vol. 93–94, p. 562. The Electrochemical Society, Pennington, NJ, 1993.
6. F. W. Poulsen, *in* "Proceedings of Third International Symposium on Ionic and Mixed Conducting Ceramics, JECS-Meeting, Sept. 1997, Paris" (M. Mogensen and T. A. Ramanarayanan, Eds.), paper # 2179 1998.
7. G. Spinolo and U. Anselmi-Tamburini, *Ber. Bunsenges. Phys. Chem.* **99,** 87 (1995).
8. G. Spinolo, U. Anselmi-Tamburini, and P. Ghigna, Z. *Naturforschung A* **52,** 629 (1997).
9. F. A. Kröger and H. J. Vink, *in* "Solid State Physics" (F. Seitz and D. Turnball, Eds.), p. 307. 1956.
10. B. C. Tofield and W. R. Scott, *J. Solid State Chem.* **10,** 183 (1974).
11. I. G. Krogh Andersen, E. Krogh Andersen, P. Norby and E. Skou, *J. Solid State Chem.* **113,** 320 (1994).
12. H. Uscida, H. Yoshikawa, T.Esaka, S. Ohtsu, and H. Iwahara, *Solid State Ionics* **36**, 89 (1989).
13. H. Iwahara, T. Yajima, T. Hibino, K. Ozaki, and H. Suzuki, *Solid State Ionics* **61**, 65 (1993).
14. T. Schober and H. Wenzl, *Ionics* **1,** 311 (1995).
15. D. Shima and S. M. Haile, *Solid State Ionics* **97,** 433 (1997).
16. E. O. Ahlgren, J. R. Hansen, N. Bonanos and F. W. Poulsen, *in* "Proceedings 17th Risø Symposium on High Temperature Electrochemistry" (F. W. Poulsen *et al.*, Eds.), p. 161 Roskilde, Denmark, 1996.
17. F. W. Poulsen and K. Wiik, in preparation.